

Experimental unilateral intracerebral hemorrhage induces delayed bilateral neurodegeneration of sciatic nerve fibres in rats

Irina M. Dovgan¹, Serhii I. Savosko¹, Alona O. Savosko², Natalia O. Melnyk¹, Alona V. Kuraieva¹, Inna V. Sokolowska³, Nataliya V. Bulgakova⁴, Yuri B. Chaikovsky^{1†}, Andriy V. Maznychenko^{3,4*}

¹ Department of Histology and Embryology, Bogomolets National Medical University, Kyiv, Ukraine,

² Department of Cytology, Histology and Reproductive Medicine, Educational and Scientific Center "Institute of Biology and Medicine", Taras Shevchenko Kyiv National University, Kyiv, Ukraine,

³ Department of Physical Education, Gdansk University of Physical Education and Sport, Gdansk, Poland,

⁴ Department of Movement Physiology, Bogomolets Institute of Physiology, Kyiv, Ukraine,

*Email: maznychenko@biph.kiev.ua

Pathological processes, such as inflammatory effects, oxidative stress, apoptosis and cytotoxicity of blood after an intracerebral hemorrhage (ICH), generally contribute to a secondary injury. One of the secondary ICH consequences in the nervous system may be delayed neurodegeneration of the peripheral nerves. Therefore, the aim of our study was to investigate possible structural changes in the sciatic nerve and changes in the conduction velocity *via* this nerve at different terms after experimental ICH in male Wistar rats. Intracerebral hemorrhage was provided by direct injection of autologous blood into the capsula interna. On the 10th day after ICH mean conduction velocity in sciatic nerve was 15% smaller compared to the control. On the 30th and 90th days after ICH, highly significant decreases in the conduction velocity by 62% and 60%, respectively in comparison with the control group of animals were observed. The data of morphometric analysis demonstrated significant decreases in the mean diameter and density of myelinated fibres at all examined terms after ICH. A number of the myelin sheaths were swollen and lost their regular laminations. Axoplasmic and myelin degenerations were the most frequent events in these nerve fibres; reductions of the diameter of the axis cylinders were also observed. In the contralateral nerve (related to the hemisphere with ICH), negative changes were greater, while the ipsilateral nerve was also subjected to those. Our data demonstrate that the consequences of unilateral ICH in the capsula interna induce bilateral negative changes in the peripheral nervous system of rats.

Key words: intracerebral hemorrhage, sciatic nerve, nerve conduction velocity, myelinated fibres, microscopy, rat

INTRODUCTION

A significant intracerebral hemorrhage (ICH) is associated with paralysis, disorders of the autonomic state and mortality (Li et al., 2017). ICH may have two main outcomes: the formation of the hematoma or hemorrhagic penetration of brain tissue. The first one often causes dislocation of anatomical brain structures, which is critical for survival. Another permeates

the brain tissue and may also be accompanied by the appearance of the hematoma. ICH is often localized in the middle cerebral artery; as a result, the pyramidal system can be damaged (Chung et al., 2000; Qureshi et al., 2003). After ICH, serious motor and sensory deficits limit daily life activities and dramatically worsen the quality of life (van Asch et al., 2010). In addition to the primary trauma induced by ICH, subsequent pathological processes, such as inflammatory effects, oxidative stress, cell death and cytotoxicity of blood generally

contribute to the secondary injury (Zhang et al., 2015). However, not only inflammation and cell death are key pathological processes responsible for the secondary brain injury after ICH; also delayed effects in the nervous system after ICH should be important pathophysiological targets for the study and further therapy (Zhao et al., 2018). Unfortunately, most studies have been focused on the death of neurons, immunocytochemical imaging of apoptosis, necrosis and demyelination with only limited descriptions (or the complete absence of information) about possible injury of the descending pathways injury (Chaudhary et al., 2015; Cao et al., 2016). Demyelination occurs not only around the site of intracerebral hemorrhage; it extends to other anatomical structures of the nervous system and includes certain time periods. The white brain matter after ICH injury was examined. Demyelination occurred inside and at the edge of the hematoma, and during about 3 days this damage spreads to the surrounding parenchyma (Wasserman et al., 2008). It has been shown that the demyelination process may last up to 2 months (Liu et al., 2010; Ni et al., 2015); i.e., further damage to the white matter inevitably develops after ICH. Also a phenomenon of the neurological deficiency, descending demyelination and changes in the activity of antioxidant enzymes in the sciatic nerve was observed in rats after ICH (Dovgan et al., 2017). The respective structural and electrophysiological changes in the peripheral nerves, however, have not been studied, although these disorders are characterized by pathophysiological manifestations in the motor centers of the cerebral cortex (Cheng et al., 2015). Hence, for effective ICH therapy, it is necessary to understand the mechanisms of the development of pathological processes occurring both in the central nervous system and in the peripheral nerve fibres.

Most often, two types of animal models of ICH are used to better understand the pathophysiology of the disease and the respective endogenous mechanisms of repair: i) infusion of a bacterial collagenase disrupts local blood vessels and produces endogenous hemorrhage into the site of injection (Masuda et al., 2010); ii) direct injection of autologous blood is performed, which causes an immediate focal hemorrhage (Brown et al., 2015). We have used an own modification of the latter model based on the introduction of autologous blood. We hypothesized that unilateral ICH is not limited by the formation of an isolated lesion of the brain structures within the site of the hemorrhage itself, but it can also lead to strong delayed bilateral disorders of myelination of peripheral nerve fibres. To confirm this hypothesis, we examined structural changes in the sciatic nerve and changes in the conduction velocity *via* this nerve at different periods (10, 30 and

90 days after ICH induced by direct injection of autologous blood in the cerebral tissue). Some part of the respective electrophysiological and morphological data has been preliminarily published (Dovgan, 2018).

METHODS

Experimental protocol

Male Wistar rats weighing 210–230 g, were used in the present study. The animals were purchased from a state-controlled animal farm through the common animal facility of the Bogomolets National Medical University (Kyiv). The experimental animals were housed in Plexiglas cages (4 rats per cage) and kept in an air-filtered, humidity- (55±5 %) and temperature-controlled (20–22°C) room with filtered air. The rats received a standard pellet diet and water *ad libitum*. The present study was approved by the Ethics Committee of the University and performed in accordance with the European Union Directive of 22 September 2010 (2010/63/EU) for the protection of animals used for scientific purposes.

The animals were divided into 5 groups (n=6 in each group): group 1 – control (intact) rats, groups 2–4 – rats after ICH examined on the 10th, 30th and 90th day, respectively and group 5 – ICH reproducibility group (group of animals used to verify the reproducibility of experimental ICH).

Hemorrhagic stroke model

Intracerebral hemorrhage in anesthetized animals (thiopental sodium, 60 mg/kg, intraperitoneally (i.p.)) was formed within a zone of the limited mechanical destruction of tissue within the right internal capsule (capsula interna dextra, L=3.5–4.0; H=6.0; AP=0.6–1.0). Such disruption was created due to 4–6 rotational movements of a “mandrin-knife”, introduced into this region with further injection into the area inside the capsule (3–4 min after destruction) of 0.2 ml of autologous blood. The latter was obtained by a standard procedure for taking blood samples from a rat (from the vein of the rats’ tail). The rat was fixed in a plastic box with a hole for the tail; the tail skin was treated with 70% ethanol. Then, an injection needle of a 1.0 ml syringe was introduced into the dorsal tail vein at the level of the middle third of the tail, and a 0.2–0.5 ml blood sample was obtained.

For mechanical destruction of the tissue inside the right internal capsule a cannula was introduced stereotactically into the rat brain. The cannula was made

from an injection needle (diameter 1.1 mm). A metal rod (mandrin from the needle for lumbar punctures) was inserted into the cannula along its entire length. The end of the mandrin was bent (the length of the bend section 0.5–0.7 mm; the bending angle 30–40°). When turning the mandrin in the cannula, the curved end of the mandrin acts as a knife (“mandrin-knife”), thereby destroying a part of the brain tissue (thus, in the area of the inner capsule, the diameter of the lesion is about 1.5 mm). After these steps, the cannula was removed. A needle without a mandrin was inserted into the brain, through which 0.2 ml of autologous blood was injected. The needle was held for up to 10 min. Local destruction of the brain in the cannula insertion zone allows to localize the injected blood volume, without blood reflux back along the cannula insertion track. Retention of the needle in the rat brain after the blood injection is necessary for blood clotting at the site of brain destruction. The blood clot is localized within the zone destroyed by the mandarin; the blood plasma is separated, forming a slight edema and the blood does not return along the cannula introduction track. Naturally, these actions cause some mechanical damage of the brain tissue, and spontaneous hemorrhage from mechanically damaged vessels of the brain also occurs, but these are no large-scale injuries. If the mandrin has not been entered, and only a one-time injection of blood is applied, then there will be a reflux of blood from the brain.

After surgery and ICH modeling, the wound on the skull region was sewn tightly by polyamide filaments 2 USP (Olympus, Ukraine) and then treated with 5% alcoholic solution of iodine.

Injury description

To measure the hematoma volume (Wang et al., 2003; Zhu et al., 2014), three 0.5 mm-thick frontal brain sections were prepared (one at the level of the cannula track and two adjacent sections with a mm step (+1 mm and –1 mm from the cannula track)). Thus, the whole hematoma volume was localized within the three slices. Then, these sections were stained with hematoxylin and eosin, and scanned on the millimeter grid, using Carl Zeiss software (AxioVision SE64 Rel.4.9.1) to trace the hematoma contour. The obtained data were summed. Results of the ICH volume measurement were as follows: on the 10th day (group 2), the respective average volume was $6.68 \pm 0.02 \text{ mm}^3$; on the 30th day (group 3) $6.80 \pm 0.04 \text{ mm}^3$, and on the 90th day (group 4) $6.54 \pm 0.04 \text{ mm}^3$. No statistically significant differences between the above groups were found.

Fig. 1 and Fig. 2 illustrate lesion areas and photomicrographs of the hemorrhage area within the rat brain sections. The hemorrhage in all cases was localized approximately in the same region, although there is some variability (Fig. 1). Fig. 2 shows that blood traces (erythrocytes) are present on the 10th day. On the 30th day, foci of injury were still visible. On the 90th day, however, a complete absence of the blood traces was observed (Fig. 2). The injury area included lacunae with multiple cells (glial cells, macrophages), which are signs of the glial scar formation. This fact can be explained by complete elimination of the products of erythrocyte destruction (hemosiderin) by macrophages.

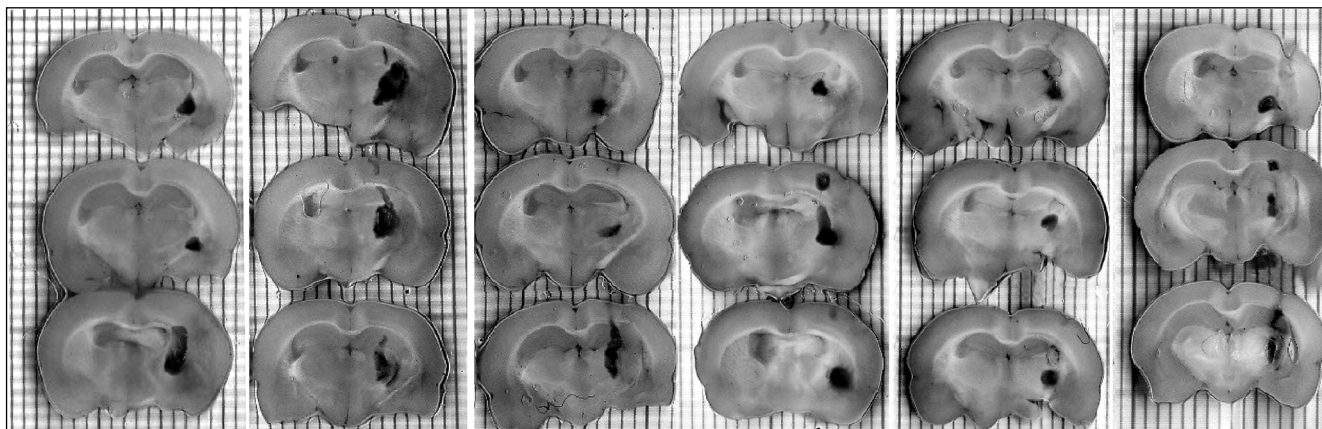


Fig. 1. Photographs of unstained brain sections of rats with injections of autologous blood illustrate the brain lesions sites (in black). Three brain sections placed vertically are presented for each animal in group 5 (n=6).

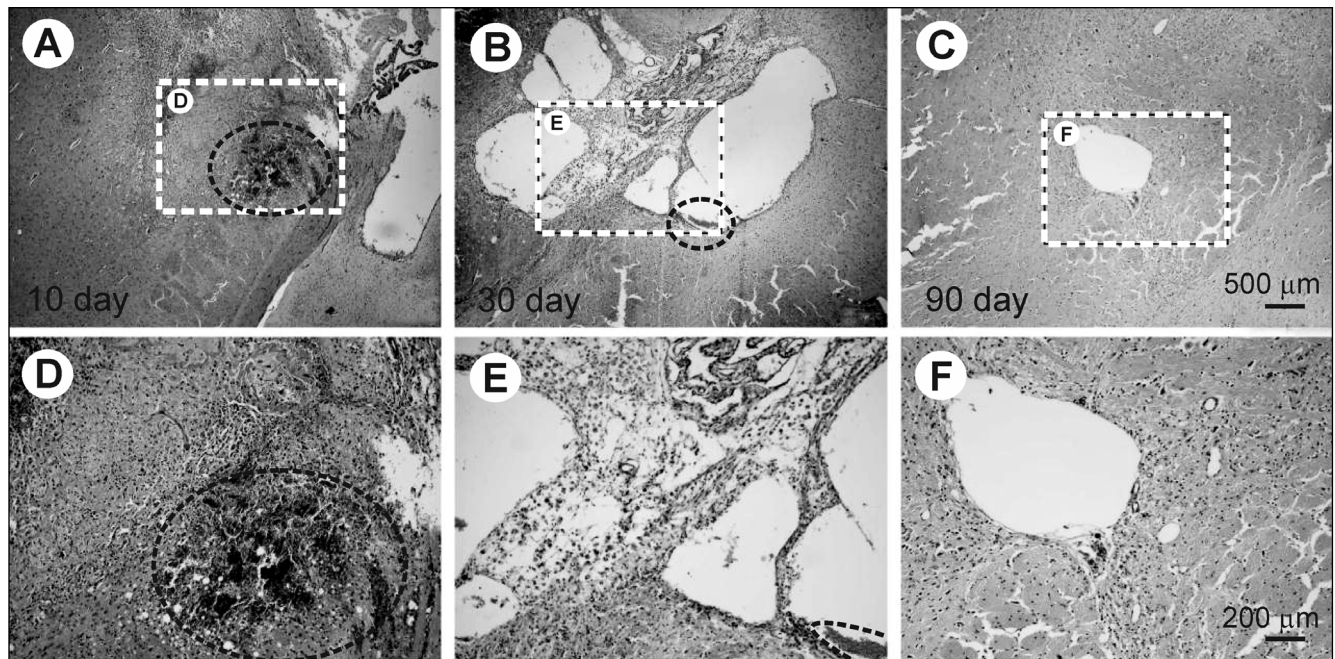


Fig. 2. Photomicrographs of rat brain sections with hemorrhage (within the internal capsule) on 10th, 30th and 90th days after stroke modeling (hematoxylin and eosin staining). On the 10th day the hemorrhage is still present, on the 30th and 90th days a lacuna is formed in the place of hemorrhage.

Inverted screen motor test

Before electrophysiological and morphological study, a modified version of the Kondziela's inverted screen test was used to measure the grip strength of the rat limbs (Kondziela, 1964; Trias et al., 2017; García-Campos et al., 2020; Badae, 2020). Rats were placed on a square wire screen (250 mm × 300 mm) with 15 mm holes, and with a soft pad placed below it. The screen was slowly inverted for 180 deg until the rats were suspended upside down on the surface of the screen. After this, the latency of falling was measured. The test was performed three times during a 30-min interval.

Electrophysiology

Control animals (group 1) and rats after 10, 30 and 90 days after ICH (groups 2–4, respectively) were used in the electrophysiological study to determinate the conduction velocity via the sciatic nerve. The animals were anaesthetized with thiopental sodium (60 mg/kg, i.p.). The sciatic nerve was separated from the surrounded tissue, its proximal part was mounted on two bipolar platinum wire electrodes for electrical stimulation, and the response (mass action potential) was recorded from the distal part. The interelectrode distance between the stimulation and recorded sites was ~30 mm. The

hindlimb muscles and nerves were covered with paraffin oil in a pool formed by the skin flaps. The pools were maintained at 37–38°C using radiant heat. The heart rate (ECG) was also continuously monitored during the experiment. Stimulation of the nerves was performed by trains of 0.2-ms long rectangular current pulses at a frequency of 3 s⁻¹ during 30 s (stimulation series). Six stimulation sessions (with 60-s rest periods between series) were applied. The stimulus intensity was set 1.3–1.5 times higher than the motor threshold. To minimize the motion during electrical stimulation, the animal's head and stimulated hindlimb were fixed to the platform. The output channels of CED (input-output interface device (CED Power 1401, UK)) generated command signals for a standard isolation unit (model DS2A, Digitimer, UK) sending stimuli to the nerves. Signals from the nerves were amplified by Brownlee model 440 amplifiers (Brownlee Precision Co., USA) and collected by a PC using the CED with 12-bit resolution at rates of 10 kHz. Data acquisition was performed using the program "Spike2" (CED).

Light and electron microscopy

After the electrophysiological study, animals were additionally anesthetized with thiopental sodium (50 mg/kg, i.p.). Identical parts of the ipsi- and contra-lateral sciatic nerves in rats of all groups were quickly

removed and fixed in a solution of 10% neutral buffered formalin (NBF, pH 7.4). Four grams of NaH_2PO_4 and 6.5 g Na_2HPO_4 were dissolved in 1.0 l of 4% formaldehyde (“Merck”, Germany) solution with distilled water to prepared 10% NBF (pH was adjusted with 1 M NaOH). Cryostat frozen longitudinal sections of the nerves (15 μm thick) were stained using silver method. Light microscopy images were optically grabbed by Olympus Microscope (Olympus BX 51). In electron microscopy (EM) study fragments of sciatic nerve were fixed in 2.5% solution of glutaraldehyde in phosphate buffer with 1% osmium tetrachloride. Dehydration was carried out in alcohols of increasing concentration (70%, 80%, 90%, 100%) and acetone. Samples of impregnated nerves were poured into a mixture of Epon-Araldite. Ultrathin sections (90 nm thick) were made using an ultratome (Reihart, Austria). Contrast was performed in 2% sodium citrate and uranyl acetate. Nerve sections were analyzed with a scanning electron microscope (Tescan Mira 3 LMU, Czech Republic).

Morphometry

The diameter of a myelinated fibers and the thickness of the myelin sheaths were measured using the CarlZeiss software (AxioVision SE64 Rel.4.9.1). For this, the values of the larger and smaller diameters of an individual fibers (since a transverse section of the nerve fiber usually has an ellipsoid shape) were measured and the mean values was calculated ((larger diameter + smaller diameter)/2). Usually, 20–50 fibers per sample were measured. The thickness of the myelin sheath was measured as the length from the border of the inner myelin lamella with the axon membrane to the outer contour of the myelin fiber.

The method of morphometric quantification of nerve fibres was based on the random selection of several test zones and their assessment in each studied nerve. First, longitudinal sections of 15 μm thickness through the length of the nerve were selected. Further, the number of nerve fibres impregnated by silver nitrate was counted under the eyepiece micrometer (magnification $\times 400$) and translated into the density per nerve thickness according to the formula. By the formula, the number of fibres in the test zone was converted to a density in mm^2 (units/test zone) (Strelin and Evsyukov, 1965; Gumenyuk et. al., 2018).

$$\text{The density of nerve fibres} = \frac{N \times 10^6}{T \times 170},$$

where N is the number of nerve fibres, T is the thickness of microsections (15 μm), and 170 is the length of test zone (170 μm).

Carl Zeiss software (AxioVision SE64 Rel.4.9.1) was used for this analysis.

Statistical analysis

The data obtained in the behavioral study are expressed as means \pm SEM. One-way ANOVA was used to analyze the values. We considered the factor of group of animals with 4 levels – intact animals, and those after ICH on the 10th, 30th and 90th day. A Bonferroni *post hoc* analysis was used to determine the differences between groups. The level of significance was set at $P < 0.05$.

Electrophysiological data were subjected to two-way statistical analysis of variance (ANOVA) and displayed graphically. Mean values \pm SEM of the conduction velocity *via* the sciatic nerves were compared in the intact animals and after ICH on the 10th, 30th and 90th day. The variation factors included two conditions: groups of animals and contra- and ipsilateral sides. A Bonferroni *post hoc* analysis was also used to determine the differences among groups. The level of intergroup differences of significance was set at $P < 0.05$.

The histological results are also expressed as means \pm SEM. The diameters in the sciatic nerve (in the right and left hindlimbs) as well as densities of nerve fibres in the same nerve samples of all rats were analyzed. Intergroup differences were evaluated by two-way ANOVA followed by the Bonferroni’s multiple comparison test. Differences of the mean values with $P < 0.05$ were considered as significant.

Before performing the ANOVA, the Shapiro-Wilk test was used to test the normality of the data distribution. At the $P > 0.05$ level, the test did not show evidence of non-normality. Homogeneity of variance was assessed using Levene’s test for equality of variances. If the P-value for Levene’s test was more than 0.05, the assumption of homogeneity of variance was considered to be met. Data analysis was performed using “Origin 8.5” (OriginLab Corporation, USA).

RESULTS

Effects of ICH on grip strength in rats

In this work, to determine the effect of experimental ICH in rats within different time periods, we evaluated the grip strength using the Kondziela’s inverted screen test in animals of all groups. A significant decrease in the motor function was observed on all studied days in

rats with experimental ICH in comparison with animals of the control group ($F_{1,34}=824.61, P<0.001, F_{1,34}=803.56, P<0.001$ and $F_{1,34}=614.02, P<0.001$, respectively). The mean latency to fall was 234.6 ± 28.2 s, 55.3 ± 8.1 s, 56.4 ± 11 s, and 77.2 ± 12.1 s in rats of the control group and on the 10th, 30th and 90th day after ICH, respectively. We used Shapiro-Wilk test to estimate normality of distribution of data in all groups of animals. It was found, the test did not show evidence of non-normality ($W=0.90, P=0.08, W=0.96, P=0.73, W=0.95, P=0.45$ and $W=0.95, P=0.54$ in 1-4 groups of animals, respectively). Additionally, we used standard Levene's test of equality of error variances for testing of homogeneity of variances (HOV) of each group of tested animals. According to the Levene's test for equality of variation (at $P>0.05$), there was homogeneity of variance for all animal groups. Note that no significant differences between values of the groups 2-4 were found ($P>0.05$) (Fig. 3).

Electrophysiology

In an electrophysiological part of the study the mean conduction velocity 35.5 ± 3.9 m/s was registered in the left sciatic nerve of the animals of the control group. The Shapiro-Wilk test did not show evidence of non-normality in data of control animals ($W=0.95, P=0.107$) as well as in animals of groups 2-4 ($W=0.95,$

$P=0.112, W=0.94, P=0.073$ and $W=0.95, P=0.133$). Ten days after ICH in rats of group 2, the mean conduction velocity via the contralateral (related to the hemisphere with ICH) sciatic nerve was by 15% lower compared to the control; nevertheless, this difference between animals of groups 1 and 2 did not reach the significance level ($F_{1,70}=3.62, P=0.061$). There was HOV for animals of these groups, as assessed by Levene's test ($F=1.97, P=0.16$). Thirty and 90 days after ICH in rats of groups 3 and 4, the mean conduction velocity was much lower compared to the control by 62% ($F_{1,70}=77.14, P<0.001$) and 60% ($F_{1,70}=58.18, P<0.001$), respectively, and these differences were statistically highly significant (Fig. 4). By the Levene's test, HOV for above animals groups were $F=4.02, P=0.072$ and $F=1.74, P=0.22$, respectively. In all cases the assumption of homogeneity of variance was considered to be met. Differences in the conduction velocity between animals of groups 3 and 4 were insignificant. It should be noted that there was no statistically significant difference in the conduction velocity via the sciatic nerve between ipsi- and contralateral nerves in the animals with ICH, as well as in intact rats.

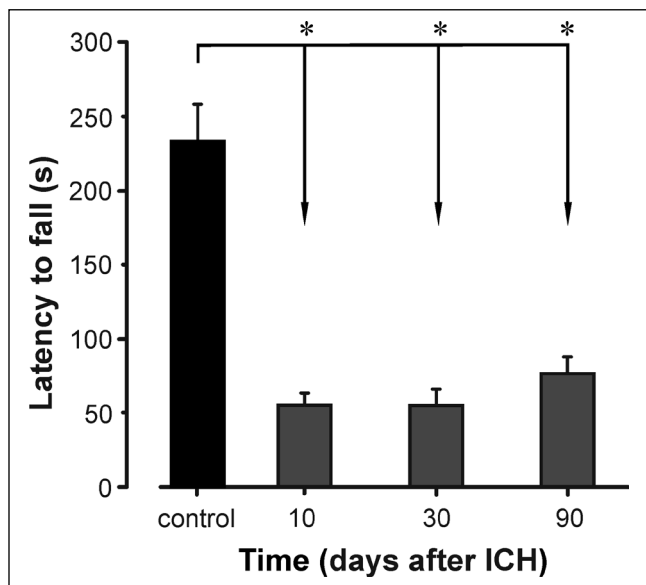


Fig. 3. A histogram of latency to fall of the control animals (black column) and rats with ICH on 10th, 30th and 90th day (grey columns), respectively. Grip strength was measured using the Kondziela's inverted screen test. Asterisks denote significant differences between control group of animals and other groups of rats ($*P<0.05$).

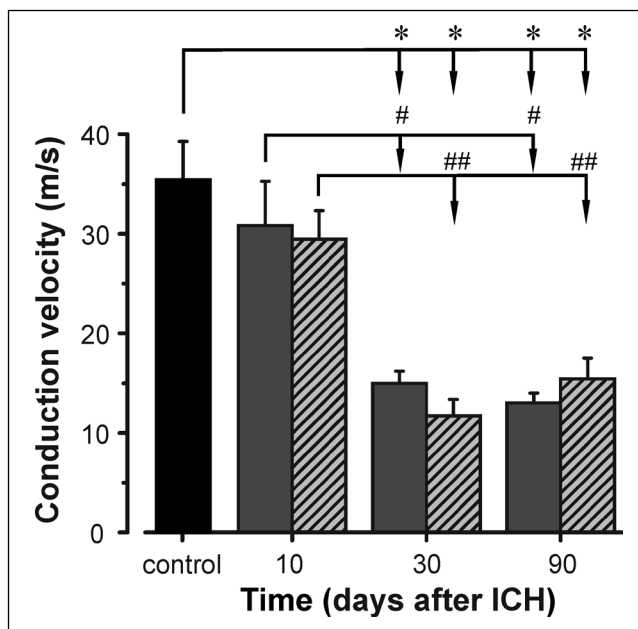


Fig. 4. Mean conduction velocity (mean ± SEM) via the sciatic nerve of the animals of the control group and rats on the 10th, 30th and 90th day after intracerebral hemorrhage (ICH). Black, dark grey and light grey (stripped) bars is conduction velocity via the unilateral nerve (in control) and in ipsi- and contralateral nerves on the 10th, 30th and 90th day, respectively. Asterisks denote significant differences in mean conduction velocity via the sciatic nerve of control animals vs. conduction velocity via the nerve of other groups of rats ($*P<0.05$); # and ## - conduction velocity via the ipsi- and contralateral nerve (respectively) of animals on 10th day after ICH vs. on 30th and 90th day after ICH ($*P<0.05, **P<0.05$).

Morphometry

The method of silver impregnation allowed us to morphologically evaluate samples of the sciatic nerve fibres. According to the data of light microscopy, the common morphological organization of the sciatic nerve in rats of groups 2 and 3 on the 10th and 30th days after ICH modeling showed no dramatic visual differences from the control (group 1). However, in the histological sections of the nerve samples obtained from these groups, bilateral decreases in the intensity of impregnation were revealed. On the 30th day, free Schwann cells were observed between nerve fibres of the ipsi- and contralateral nerves in animals of group 3. This phenomenon may be a manifestation of dedifferentiation of the Schwann cells on the background of degeneration of the nerve fibres. In addition, local swellings were observed, mainly within the areas close to the nodes of Ranvier (Fig. 5A–D). The data of morphometric analysis showed that the mean diameter and density of myelinated fibres in the experimental groups 2 and 3 were significant decreased. The diameter of nerve fibres in groups of animals 2 and 3 were ~20% less in comparison with the control (Table 1), and the density of such fibres was ~27% less compared to that in group 1 (Table 1). On the 90th day in rats of group 4, in addition to a decrease in the level of impregnation (Fig. 5E, 5F), significant decreases in the mean diameter of nerve fibres by 39.5% and 47.5% (ipsi- and contralaterally) and decreases in the mean density by 41.8% and 71.5% (ipsi- and contralaterally, relative to the side of the ICH, Table 1) were observed. This was especially noticeable in the contralateral sciatic nerve. It should be noted that paresis of the left (contralateral) hind-limb developed on the 90th day in animals of the fourth group. In animals with limb paresis, individual fascicles were observed, with the absence of nerve fibres were found; those contained only neurolemmocytes, perineurium, and blood vessels. The products of degenerated nerve fibers decay and infiltrating macrophages

were no longer observed, indicating their complete elimination in terms of 30 to 90 days. This fact may be an additional confirmation of structural disorders of the pyramidal tract.

Electron microscopic examination was additionally carried out to confirm the hypothesis of delayed neurodegeneration. Ultrastructure changes in myelinated nerve fibres were investigated. On the 10th day after ICH, a notable axonal pathology was not observed. One month after ICH, however, various lesions of axonal structures (axial cylinders and myelin sheath) were observed. A lot of myelin sheaths looked to be swollen and lost their regular laminations. Axoplasmic and myelin degeneration was the most frequent finding in these nerve fibres. Various vesicles and osmophilic corpuscles in the axoplasm were observed, and a reduction of the diameter of the axis cylinders was obvious (Fig. 6). Such injuries became more intense as the ICH consequences progressed.

The analysis of the ultrastructure myelinated nerve fibres demonstrated a variable pattern of the changes. A significant resistivity of the axial cylinders to damage was noted, an increase in the mean diameter of axial cylinders was observed in a small number of myelinated fibres (1.23±0.06 µm in the contralateral nerve and 1.18±0.05 µm in the ipsilateral nerve vs. 0.90±0.03 µm in the control nerve, P<0.05). It should be noted that serious abnormalities in non-myelinated fibres (such as atrophy) were not observed. In all cases of morphological assessments, data normality test did not show evidence of non-normality (P>0.05) and HOV was considered to be met (P>0.05).

DISCUSSION

In our experimental model with the above-described technique of damage of the internal capsule there are several pathological factors, namely acute mechanical destruction and injection of autologous

Table 1. Changing the mean diameter and density of myelinated fibres of the sciatic nerve after ICH.

Groups	Mean fibres diameters, µm		Mean fibres density, units/test-zone	
	contralateral nerve	ipsilateral nerve	contralateral nerve	ipsilateral nerve
Control	8.17±0.19 (unilaterally)		10980.35±78.4 (unilaterally)	
10 days after ICH	6.33±0.13*	6.50±0.14*	7647±58.82*	8823.5±98.4*
30 days after ICH	6.35±0.15*	7.21±0.18***	7447±61.82*	8235.3±117.6***
90 days after ICH	4.29±0.12*	5.67±0.15***	3137.1±68.6*	6274±58.3***

Two-way ANOVA was used to calculate mean diameter or density of myelinated fibres. * P<0.05 – between nerve fibres diameters/density in animals after ICH and control group; ** P<0.05 – between ipsi- and contralateral nerve in the same group.

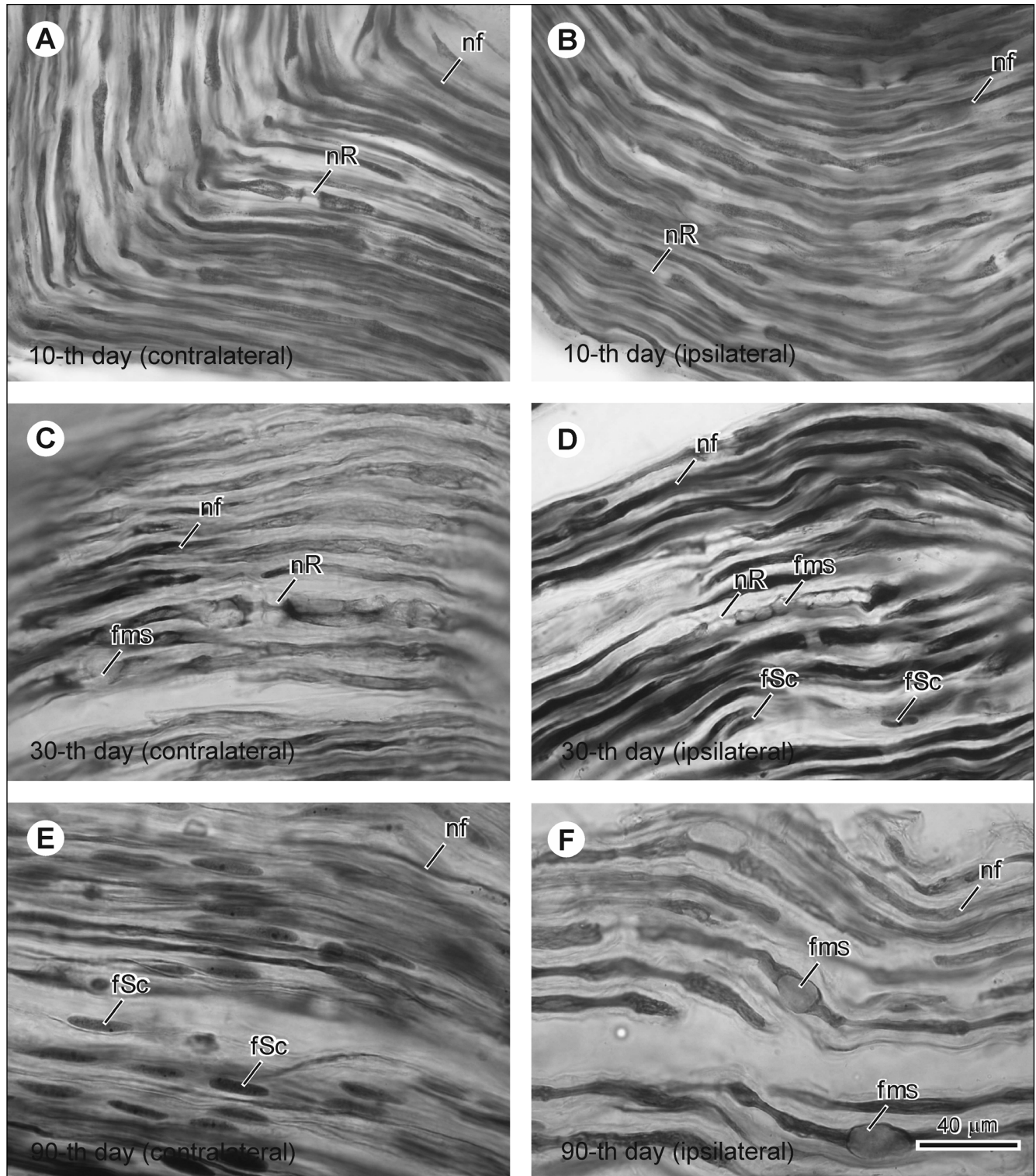


Fig. 5. Photomicrographs of silver impregnated sciatic nerve fibres of rats, on the 10th day (A, B), 30th day (C, D) and 90th day (E, F) after intracerebral hemorrhage (ICH). Left column (A, C, E) corresponds to the left or contralateral (related to hemisphere with ICH) sciatic nerve; right column (B, D, F) – ipsilateral (right) sciatic nerve. fms – focal myelin swelling; fSc – free Schwann cell; nf – nerve fibre; nR – node of Ranvier. Scale bar 40 µm on (F) also appreciated for (A–E).

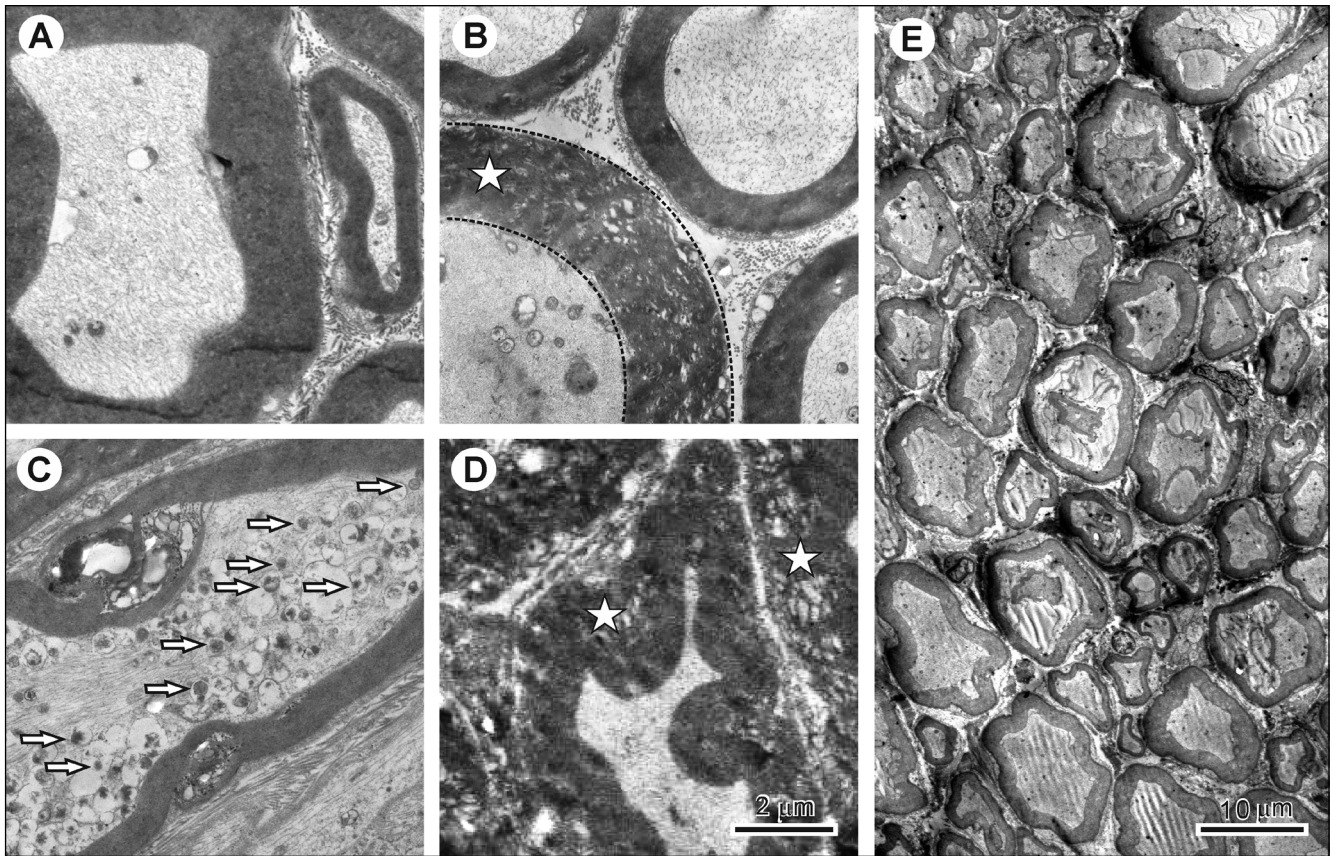


Fig. 6. Scanning electron microscopy images of right sciatic nerve samples in control (A), on 10th day (B), 30th day (C) and 90th day (D) after intracerebral hemorrhage (ICH). Sciatic nerve on 10th day after ICH with low magnification is presented in (E). Asterisks in (B, D) show degenerating myelin (local swellings). White arrow in (C) indicates on various vesicles and osmophilic corpuscles in the axoplasm arrows. Scale bars: 2 µm for D (also appreciated for A–C) and 10 µm for (E).

blood into this site. From our own experience and various described modifications of the experiments (Makarenko et al., 2013; Savosko et al., 2013) we have concluded that both these factors cause damage of the white and gray matter of the brain (including neuronal degeneration, brain edema, angionecrosis, and migration of macrophages, microglia, and neutrophils to the damage site). As is known, a mechanical injury is always accompanied by local hemorrhage, but to standardize the latter (standard blood volume, hemorrhage topography) we additionally introduce autologous blood. After such manipulation, blood reflux does not occur *via* the needle track, and there is no need to re-inject the blood for correction of the hematoma volume as described by Yang et al. (1994) and Deinsberger et al. (1996). That's why local brain damage in our model can be extrapolated to the study of some pathophysiological aspects of acute mechanical trauma, brain hemorrhage, and combined trauma with hemorrhage, as shown in the studies on subcortical capsular infarcts and intracerebral hemorrhage (Ma et al., 2011; Kim et al., 2014; Katsuki and Hijioka,

2017). A method of reproduction of a spontaneous intracerebral hemorrhage has not been invented yet. So, all experimental models are related to at least a minimal traumatic factor, although Lee and coauthors described spontaneous intracerebral hemorrhages in SHRSP male rats using modified high-salt low-protein “Japanese-style” diet; these hemorrhages, however, were unpredictable in their localization and volume (Lee et al., 2007).

In our experiments, the track of the cannula (needle), through which the internal capsule was destroyed, and blood was injected, partially damaged the somatosensory cortex. Paresis of the hindlimb occurred after significant damage to the internal capsule, and it appeared to be a successful way to damage many components of the corticospinal tract. We have found that mechanical destruction of the internal capsule as a simple way to induce degenerative changes in the corticospinal tract, similar to those after focal introduction of malonate, ouabain or endothelin-1; such intervention results in a partial loss of mobility of the contralateral limb (Janowski et al., 2008; Lec-

rux et al., 2008; Blasi et al., 2015; Cirillo et al., 2018). Primary lesion of the internal capsule (destruction of axons and demyelination after a mechanical damage, soaking of the brain with blood) is combined with secondary damage of the corticospinal pathways by products of hemolysis and degradation of heme. This makes impossible transmission of the descending signals *via* the spinal cord, thereby causing hemiparesis (Katsuki and Hijioka, 2017). A secondary damage (atrophy) progresses with the increase of synthesis of proinflammatory factors (leukotriene B4, IL-1 β , IL-6) and appearance of neutrophils stimulated by chemotaxis in the hemorrhage zone (Hijioka et al., 2017). This is proved by progressive rostrocaudal Wallerian degeneration and poor functional outcome in stroke patients in three months (Venkatasubramanian et al., 2013). In our experiments, suppression of locomotor activity was delayed and progressing. Those also were the features of gradual loss of nerve fibres in the sciatic nerve, which was an obvious result of secondary damage after a hemorrhage in the internal capsule.

In our study, the inverted screen motor test has been used to assess the motor deficits in rats with ICH. Recently, this test was used in rats with intracerebral haemorrhage after atorvastatin intake (Badae, 2020), in those animals with modeled amyotrophic lateral sclerosis (Trias et al., 2017), and in mice with an impaired muscle function (García-Campos, 2020). In those studies, there was a significant variability of the latent period of negative symptoms in the animals, apparently due to the peculiarities of the test in each particular study. For example, Badae (2020) in his work noted that the grip strength and muscle force in animals after intracerebral hemorrhage were partially recovered in the first day and then within a week, remained almost unchanged. Although the experiment in Badae's work lasted only a week, in our study we found a similar pattern of the functional changes.

It is known that the silver nitrate impregnation technique is effectively used to investigate the architecture of axons (Lourbopoulos et al., 2007; Goebels et al., 2010; Nauta and Ebesson, 2012). It is also known that myelin degeneration is the most frequent injuries in the nerve fibres (Wasserman et al., 2008). A Schwann cell forms a myelin sheath by wrapping its plasma membrane concentrically around the inner axon. Approximately 30% protein and about 70% hydrophilic phospholipids and glycolipids compose myelin (Kiernan, 2007). To preserve of the protein-lipid structure of myelin it is necessary to use a frozen sections because solvents used in paraffin processing extract most lipids (Kiernan, 2007). Hence, among the possible research methods, the silver impregnation technique (with using freezing process for cut-

ting-sections) is appropriate for this type of the study and for the objective.

The results of electrophysiological and morphological studies confirm the development of demyelination and degeneration of nerve fibres of the sciatic nerve in studied terms. In the view of the decrease in the conduction velocity *via* the nerve and the significant loss of nerve fibres on the 30th day, it is assumed that the latter term (30 days) is a critical period, after which neurodegenerative changes in the nerve begin to progress more rapidly. The results of electrophysiological studies showed a significant decrease in the mean conduction velocity on the 30th and 90th day after the ICH in comparison with the control. One of the factors influencing the conduction velocity through the nerve may be structural changes in the axons and a resulting decrease in the diameters of the latter. Also, these modifications should be related to the failures in the process of formation of the cytoskeletal structures and a slowdown of transport of the neurofilaments. Apparently, these effects are based on metabolic shifts, in particular intensification of non-enzymatic glycosylation and malfunctions of phosphorylation of structural proteins in the injured neurons (Kostyuk et al., 1996). Furthermore, local swellings, which have been observed in the nerve filaments, may also be an additional factor responsible for a decrease in the conduction velocity. These changes lead to degeneration of the nerve fibres, first of all to damage to myelin sheaths of the latter. Ultrastructural manifestations of these changes are swellings, deformation of the myelin sheath, and detachment of myelin from the axon. It can be ruled out that demyelination is an early phase in the degeneration of the entire neuron, and it will, in the future, result in atrophy of the fibres or Wallerian degeneration. Kolaric et al. (2013) in his study demonstrated that single swellings accompanied by demyelination of the swollen region attenuate the conduction, whereas multiple swellings in similarly demyelinated axons demonstrated greater slowing down of the conduction at equivalent dimensions of single swellings. Increasing axolemmal permeability greatly decreased the dimensions of a swelling that resulted in conduction block. It was suggested that the most important factor that leads to the conduction block in swollen axons is not swelling per se or accompanying demyelination, but the increased axonal permeability, which acts as a transmembrane current shunt.

In rabbit studies, Gundogdu et al. (2008) identified left sciatic nerve hemiplegia in 8 of 10 animals with intracerebral hemorrhage in the right sensorimotor cortex. Degenerated axons, myelin sheath abnormalities, and loss of axons were detected in the left L3

ventral spinal root. A decrease in the number of endothelial cell nuclei in the arteries (arterial nervorum) of the sciatic nerve was observed. The authors consider the causal relations of the arterial factor with degeneration of nerve fibers in the nerve. Structural and functional changes in the nerve vessels after intracerebral hemorrhage can lead to a significant sciatic nerve damage.

It has also been shown that vasospasm in the spinal cord (Adamkiewicz artery branches) after spinal subarachnoid hemorrhage can lead to injury of the third and second sensory neurons of the spinal cortical sensory pathways and finally lead to neurodegeneration (apoptosis and necrosis) of dorsal root ganglia (Ozturk et al., 2015). Degeneration of the nerve endings that regulate blood flow in the peripheral nerve (particularly in the perivascular autonomic nerve plexus) can lead to serious disorders of endoneurial blood flow and nerve damage (Teunissen et al., 2002).

In our work, a decrease in the diameter of myelinated nerve fibres in the sciatic nerve was registered throughout the study period. Main changes were noted in the contralateral nerve in relation to the hemisphere with ICH, but changes in the ipsilateral nerve were also significant. Contralateral lesions in the peripheral nervous system were anticipated because 80–95% of the corticospinal tract fibers are crossed in the medulla oblongata and run dorsomedially and dorsolaterally in the rat spinal cord (Lacroix et al., 2004; Rosenzweig et al., 2009). Morphological and functional changes of the ipsi- and contralateral sciatic nerve described in the above article, are obvious causes of bilateral decreases in the conductivity through the peripheral nerve of the limbs after a pyramidal tract injury (Chroni et al., 2007; Paoloni et al., 2010; Hunkar and Balci, 2012). Earlier, Schmalbruch (1986) examined the sciatic nerve of rats and found that a vast majority of the unmyelinated nerve fibres are afferent. This may explain the fact that intact unmyelinated fibers found in the sciatic nerve (in the case of an injured pyramidal tract and degenerated myelinated fibres) are obviously efferent. These data demonstrate that bilateral changes in the peripheral nervous system apparently are the result of unilateral ICH.

CONCLUSION

Thus, our study showed that local unilateral brain injury using a model of hemorrhagic stroke in rats can induce time-delayed strong structural and functional changes in the sciatic nerve, which lead to bilateral degeneration of peripheral nerve fibres.

REFERENCES

- Badae N, Zahran N, Baraka A, Elshinety R, Dief A (2020) Functional and morphological consequences after atorvastatin intake in a rat model of intracerebral haemorrhage. *Bull Egypt Soc Physiol Sci* 40: 86–102.
- Blasi F, Whalen MJ, Ayata C (2015) Lasting pure-motor deficits after focal posterior internal capsule white-matter infarcts in rats. *J Cereb Blood Flow Metab* 35: 977–984.
- Brown RJ, Epling BP, Staff I, Fortunato G, Grady JJ, McCullough LD (2015) Polyuria and cerebral vasospasm after aneurysmal subarachnoid hemorrhage. *BMC Neurol* 15: 201.
- Cao S, Zheng M, Hua Y, Chen G, Keep RF, Xi G (2016) Hematoma changes during clot resolution after experimental intracerebral hemorrhage. *Stroke* 47: 1626–1631.
- Chaudhary N, Pandey AS, Gemmete JJ, Hua Y, Huang Y, Gu Y, Xi G (2015) Diffusion tensor imaging in hemorrhagic stroke. *Exp Neurol* 272: 88–96.
- Cheng CY, Hsu CY, Huang YC, Tsai YH, Hsu HT, Yang WH, Lin HC, Wang TC, Cheng WC, Yang JT, Lee TC, Lee MH (2015) Motor outcome of deep intracerebral haemorrhage in diffusion tensor imaging: comparison of data from different locations along the corticospinal tract. *Neurol Res* 37: 774–781.
- Chroni E, Argyriou AA, Katsoulas G, Polychronopoulos P (2007) Ulnar F wave generation assessed within 3 days after the onset of stroke in patients with relatively preserved level of consciousness. *Clin Neurol Neurosurg* 109: 27–31.
- Chung CS, Caplan LR, Yamamoto Y, Chang HM, Lee SJ, Song HJ, Lee HS, Shin HK, Yoo KM (2000) Striatocapsular haemorrhage. *Brain* 123: 1850–1862.
- Cirillo C, Le Fric A, Frisach I, Darmana R, Robert L, Desmoulin F, Loubinoux I (2018) Focal malonate injection into the internal capsule of rats as a model of lacunar stroke. *Front Neurol* 9: 1072.
- Deinsberger W, Vogel J, Kuschinsky W, Auer LM, Böker DK (1996) Experimental intracerebral hemorrhage: description of a double injection model in rats. *Neurol Res* 18: 475–477.
- Dovgan IM, Melnyk NO, Labunets IF, Utiko NA, Savosko SI (2017) The activity of antioxidant enzymes in rat sciatic nerve following a hemorrhagic stroke. *World Med Biol* 3: 100–117.
- Dovgan IM (2018) Structural and electrophysiological changes in sciatic nerve after intracerebral hemorrhage in rats. *Fiziol Zh* 64: 91–98.
- García-Campos P, Báez-Matus X, Jara-Gutiérrez C, Paz-Araos M, Astorga C, Cea LA, Rodríguez V, Bevilacqua JA, Cavedes P, Cárdenas AM (2020) N-acetylcysteine reduces skeletal muscles oxidative stress and improves grip strength in dysferlin-deficient Bla/J mice. *Int J Mol Sci* 21: 4293.
- Goebbels S, Oltrogge JH, Kemper R, Heilmann I, Bormuth I, Wolfer S, Wichert SP, Möbius W, Liu X, Lappe-Siefke C, Rossner MJ, Groszer M, Suter U, Frahm J, Boretius S, Nave KA (2010) Elevated phosphatidylinositol 3,4,5-trisphosphate in glia triggers cell-autonomous membrane wrapping and myelination. *J Neurosci* 30: 8953–8964.
- Gumenyuk A, Rybalko S, Ryzha A, Savosko S, Labudzynski D, Levchuk N, Chaikovskiy Yu (2018) Nerve regeneration in conditions of HSV-infection and an antiviral drug influence. *Anat Rec* 301: 1734–1744.
- Gundogdu C, Aydin MD, Kotan D, Aydin N, Bayram E, Ulvi H, Aygul R (2008) Vascular mechanism of axonal degeneration in peripheral nerves in hemiplegic sides after cerebral hemorrhage: An experimental study. *J Brachial Plex Peripher Nerve Inj* 3: 13.
- Hijioka M, Anan J, Ishibashi H, Kurauchi Y, Hisatsune A, Seki T, Koga T, Yokomizo T, Shimizu T, Katsuki H (2017) Inhibition of leukotriene B4 action mitigates intracerebral hemorrhage-associated pathological events in mice. *J Pharmacol Exp Ther* 360: 399–408.
- Hunkar R, Balci K (2012) Entrapment neuropathies in chronic stroke patients. *J Clin Neurophysiol* 29: 96–100.
- Janowski M, Gornicka-Pawlak E, Kozłowska H, Domanska-Janik K, Gielecki J, Lukomska B (2008) Structural and functional characteristic

- of a model for deep-seated lacunar infarct in rats. *J Neurol Sci* 273: 40–48.
- Katsuki H, Hijioka M (2017) Intracerebral hemorrhage as an axonal tract injury disorder with inflammatory reactions. *Biol Pharm Bull* 40: 564–568.
- Kiernan JA (2007) Normal and degenerating myelin in the central and peripheral nervous systems. *J Histotechnol* 30: 87–106.
- Kim HS, Kim D, Kim RG, Kim JM, Chung E, Neto PR, Lee MC, Kim HI (2014) A rat model of photothrombotic capsular infarct with a marked motor deficit: a behavioral, histologic, and microPET study. *J Cereb Blood Flow Metab* 34: 683–689.
- Kolaric KV, Thomson G, Edgar JM, Brown AM (2013) Focal axonal swellings and associated ultrastructural changes attenuate conduction velocity in central nervous system axons: a computer modeling study. *Physiol Rep* 1: e00059.
- Kondziela W (1964) Eine neue method zur messung der muskularen relaxation bei weissen mausen. *Arch Int Pharmacodyn* 152: 277–284.
- Kostyuk EP, Bulgakova NV, Vasilenko DA (1996) Parameters of conduction via afferent nerve fibres in mice with streptozotocin-induced and genetically determined diabetes. *Neurophysiol* 28: 135–139.
- Lacroix S, Havton L, McKay H, Yang H, Brant A, Roberts J, Tuszynski MH (2004) Bilateral corticospinal projections arise from each motor cortex in the macaque monkey: a quantitative study. *J Comp Neurol* 473: 147–161.
- Lecrux C, McCabe C, Weir CJ, Gallagher L, Mullin J, Touzani O, Muir KW, Kennedy R, Lees I, Macrae M (2008) Effects of magnesium treatment in a model of internal capsule lesion in spontaneously hypertensive rats. *Stroke* 39: 448–454.
- Lee J, Zhai G, Liu Q, Gonzales ER, Yin K, Yan P, Hsu CY, Vo KD, Lin W (2007) Vascular permeability precedes spontaneous intracerebral hemorrhage in stroke-prone spontaneously hypertensive rats. *Stroke* 38: 3289–3291.
- Lourbopoulos A, Grigoriadis S, Symeonidou C, Deretzi G, Taskos N, Shohami E, Grigoriadis N (2007) Modified Beilschowsky silver impregnation combined with Hematoxylin or Cresyl Violet counterstaining as a potential tool for the simultaneous study of inflammation and axonal injury in the central nervous system. *Aristotle Univ Med J* 34: 31–39.
- Li X, Cao R, Lu H, Tian W, Yu N, Zhang P, Dong Z (2017) Cerebral hemorrhage therapy by targeting VEGF and HGF in a preclinical trial in rats. *Mol Med Rep* 15: 3093–3098.
- Liu AM, Lu G, Tsang KS, Li G, Wu Y, Huang ZS, Keung NH, Kung KF, Sang PW (2010) Umbilical cord-derived mesenchymal stem cells with forced expression of hepatocyte growth factor enhance remyelination and functional recovery in a rat intracerebral hemorrhage model. *Neurosurgery* 67: 365–366.
- Ma Q, Khatibi N, Chen H, Tang J, Zhang JH (2011) History of preclinical models of intracerebral hemorrhage. *Acta Neurochir Suppl* 111: 3–8.
- Makarenko A, Morozov S, Savosko S, Vasil'eva IG (2013) Simulation of repeated local hemorrhagic stroke in rats. *Patol Fiziol Eksp Ter* 1: 81–85.
- Masuda T, Maki M, Hara K, Yasuhara T, Matsukawa N, Yu S, Bae EC, Tajiri N, Chheda SH, Solomita MA, Weinbren N, Kaneko Y, Kirov SA, Hess DC, Hida H, Borlongan CV (2010) Peri-hemorrhagic degeneration accompanies stereotaxic collagenase-mediated cortical hemorrhage in mouse. *Brain Res* 1355: 228–239.
- Nauta WJH, Ebbesson SOE (2012) Contemporary Research Methods in Neuroanatomy: Proceedings of an International Conference held at the Laboratory of Perinatal Physiology, San Juan, Puerto Rico, in January 1969 under the auspices of the National Institute of Neurological Diseases and Stroke and the University of Puerto Rico. Springer Science and Business Media.
- Ni W, Okauchi M, Hatakeyama T, Gu Y, Keep RF, Xi G, Hua Y (2015) Deferoxamine reduces intracerebral hemorrhage-induced white matter damage in aged rats. *Exp Neurol* 272: 128–134.
- Ozturk C, Kanat A, Aydin MD, Yolas C, Kabalar ME, Gundogdu B, Duman A, Kanat IF, Gundogdu C (2015) The impact of L5 dorsal root ganglion degeneration and Adamkiewicz artery vasospasm on descending colon dilatation following spinal subarachnoid hemorrhage: An experimental study; first report. *J Craniovertebr Junction Spine* 6: 69–75.
- Paoloni M, Volpe B, Mangone M, Ioppolo F, Santilli V (2010) Peripheral nerve conduction abnormalities in nonparetic side of ischemic stroke patients. *J Clin Neurophysiol* 27: 48–51.
- Qureshi AI, Ali Z, Suri MF, Shuaib A, Baker G, Todd K, Lee G, Hopkins L (2003) Extracellular glutamate and other amino acids in experimental intracerebral hemorrhage: an in vivo microdialysis study. *Crit Care Med* 31: 1482–1489.
- Rosenzweig E, Brock J, Culbertson M, Lu P, Moseanko R, Edgerton VR, Havton LA, Tuszynski MH (2009) Extensive spinal decussation and bilateral termination of cervical corticospinal projections in rhesus monkeys. *J Comp Neurol* 513: 151–163.
- Savosko S, Chaikovsky Ju, Pogorela N, Makarenko AN (2013) Features of histostructural changes in rat cerebral cortex in hemorrhagic stroke modeling. *Int J Phys Pathophys* 4: 113–121.
- Strelin GS, Evsyukov VI (1965) On suppression and restoration of the ability to regenerate the peripheral nerve after irradiation. *Med Radiol Radiat Safety* 10: 67–73.
- Schmalbruch H (1986) Fiber composition of the rat sciatic nerve. *Anat Rec* 215: 71–81.
- van Asch CJ, Luitse MJ, Rinkel GJ, van der Tweel I, Algra A, Klijn CJM (2010) Incidence, case fatality, and functional outcome of intracerebral haemorrhage over time, according to age, sex, and ethnic origin: a systematic review and meta-analysis. *Lancet Neurol* 9: 167–176.
- Teunissen LL, Veldink J, Notermans NC, Bleyers RL (2002) Quantitative assessment of the innervation of epineurial arteries in the peripheral nerve by immunofluorescence: differences between controls and patients with peripheral arterial disease. *Acta Neuropathol* 103: 475–480.
- Trias E, Ibarburu S, Barreto-Núñez R, Varela V, Moura IC, Dubreuil P, Hermine O, Beckman JS, Barbeito L (2017) Evidence for mast cells contributing to neuromuscular pathology in an inherited model of ALS. *JCI Insight* 2: e95934.
- Venkatasubramanian C, Kleinman J, Fischbein N, Olivot JM, Gean AD, Eyngorn I, Snider RW, Mlynash M, Wijman CAC (2013) Natural history and prognostic value of corticospinal tract Wallerian degeneration in intracerebral hemorrhage. *J Am Heart Assoc* 2: e000090.
- Wang J, Rogove AD, Tsirka AE, Tsirka SE (2003) Protective role of tuftsin fragment 1-3 in an animal model of intracerebral hemorrhage. *Ann Neurol* 54: 655–664.
- Wasserman JK, Schlichter LC (2008) White matter injury in young and aged rats after intracerebral hemorrhage. *Exp Neurol* 214: 266–275.
- Yang G, Betz A, Chenevert T, Brunberg J, Brunberg JA, Hoff JT (1994) Experimental intracerebral hemorrhage: relationship between brain edema, blood flow, and blood-brain barrier permeability in rats. *J Neurosurg* 81: 93–102.
- Zhang Y, Yi B, Ma J, Zhang L, Zhang H, Yang Y, Dai Y (2015) Quercetin promotes neuronal and behavioral recovery by suppressing inflammatory response and apoptosis in a rat model of intracerebral hemorrhage. *Neurochem Res* 40: 195–203.
- Zhao H, Chen Y, Feng H (2018) P2X7 Receptor-associated programmed cell death in the pathophysiology of hemorrhagic stroke. *Curr Neuropharmacol* 16: 1282–1295.
- Zhu W, Gao Y, Chang CF, Wan JR, Zhu SS, Wang J (2014) Mouse models of intracerebral hemorrhage in ventricle, cortex, and hippocampus by injections of autologous blood or collagenase. *PLoS One* 9: e97423.